Electronic Supplementary Material (ESI) for Nanoscale.
This journal is © The Royal Society of Chemistry 2017

Supporting information for

Tuning the collective switching behavior of azobenzene/Au hybrid materials: flexible versus rigid azobenzene backbone and Au(111) surface versus highly curved nanoparticle

Chunyan Liu, Dong Zheng, Weigang Hu, Qiang Zhu, Ziqi Tian, Jun Zhao, Yan Zhu*

and Jing Ma*

Key Laboratory of Mesoscopic Chemistry of MOE, School of Chemistry & Chemical Engineering, Nanjing University 22 Hankou Road, Nanjing, 210093, People's Republic of China

List of content

1. Potential energy curve of inversion path and comparison of the calculated spectra with experiment

(a)

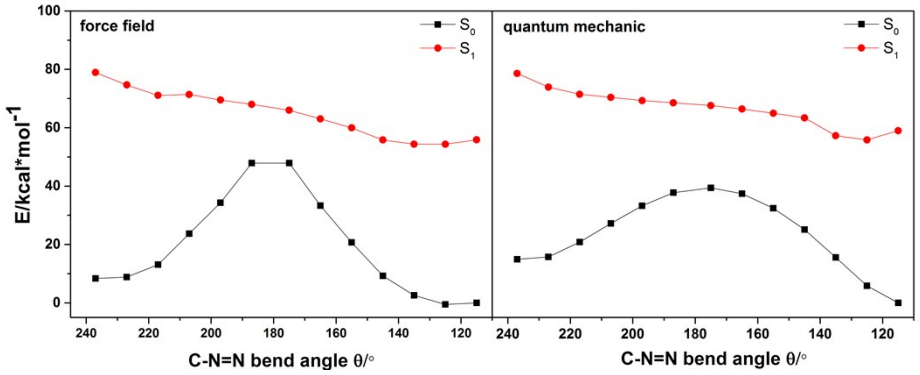

(b)

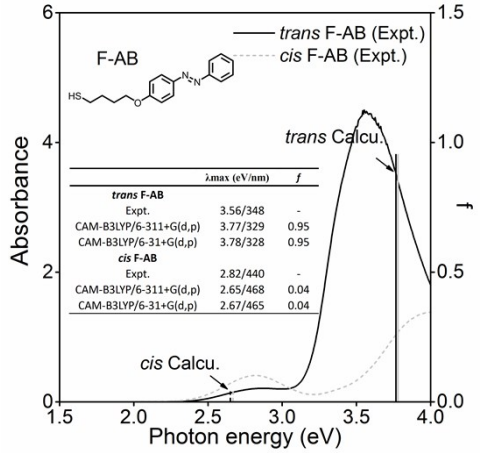

(c)

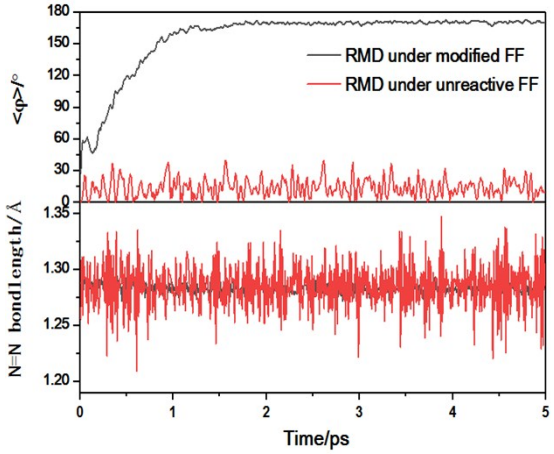

Figure S1. (a) Potential energy curve along the inversion path for azobenzene under the quantum mechanics and force fields; (b); comparison made between the calculated spectra (column) and experimental UV-Vis spectra (curve, concentration: 4.0×10^{-6}M) of *trans* or *cis* F-AB; and the TDDFT computational levels are CAM-B3LYP/6-311+G(d,p) and CAM-B3LYP/6-31+G(d,p), respectively. (c) illustration of the unreactive *versus* reactive MD trajectories.

Under default parameters on C-N=N-C torsion term and C-N=N bend term within various classical force fields (such as CVFF, PCFF, CHARMM36), the switching behavior of azobenzene is not observed, illustrated as the following dynamic process (red lines in Figure S1c) of a single R-AB in gas phase. Hence, the default parameters is described as "unreactive".

Based on the accurate C-N=N-C torsion and C-N=N bend potential energy curve through QM calculation (Figure S1a), the corresponding parameter is properly modified within standard forcefield framework and reproduce the potential energy curve. After the modification, the successful switching behavior (black lines in Figure S1c) of azobenzene is well described. During the switching process from *cis* to *trans*, the N=N bond demonstrates minor change and do not involve bond breaking. Compared to results under default forcefield, the modified one is "reactive".

2. Experiments of F-AB and A_{25}@F-AB

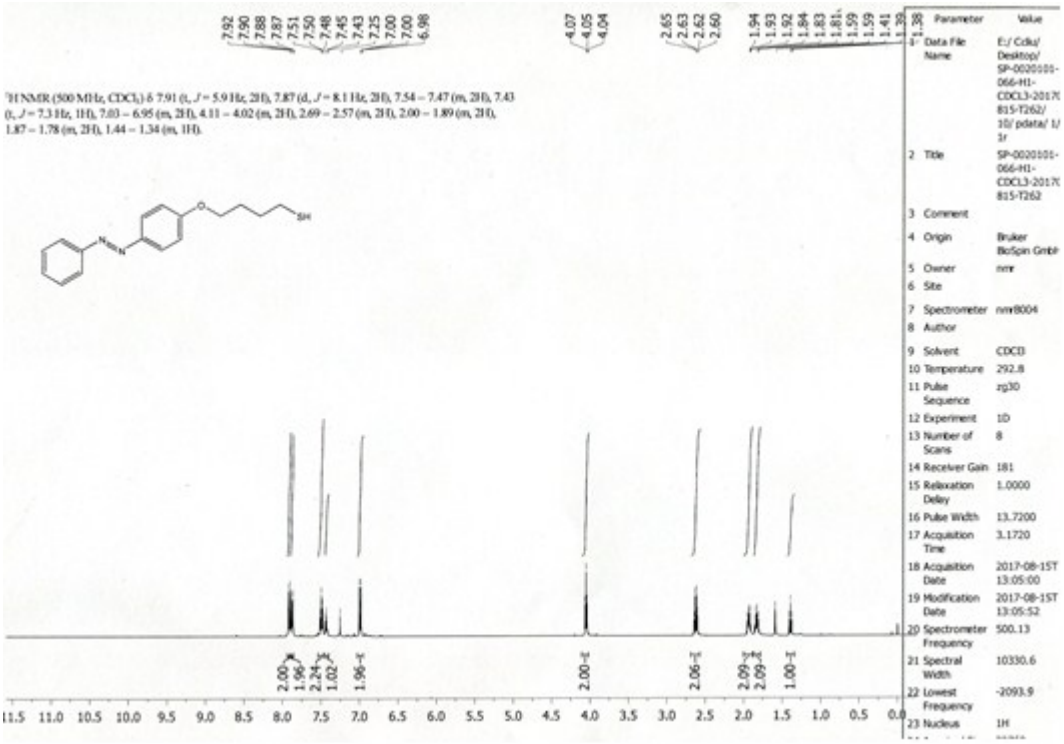

Figure S2. ^{1}H nuclear magnetic resonance (NMR) spectrum of F-AB (also called Az-SH in literature), NMR analysis was conducted on Bruker Biospingmbl spectrometer. The data was collected with a sample in $CDCl_3$.

The kinetics of thermal *cis-to-trans* relaxation is calculated from Eq. S1

$$\ln \frac{A_0 - A_\infty}{A_t - A_\infty} = k_r \times t \qquad \text{(S1)}$$

Where k_r is the rate constant of the *cis-to-trans* thermal relaxation and t is the reaction time. The values of A_0, A_t, and A_∞ are the absorbances corresponding to the time 0 (in *cis* form), t, and photo-stationary state (∞), as shown in Fig. 2c and 2d. The results are shown in Figure S3. The thermal isomerization of F-AB in Au_{25}@F-AB is slightly slower than that of free F-AB with a relative isomerization time ratio of 1.1.

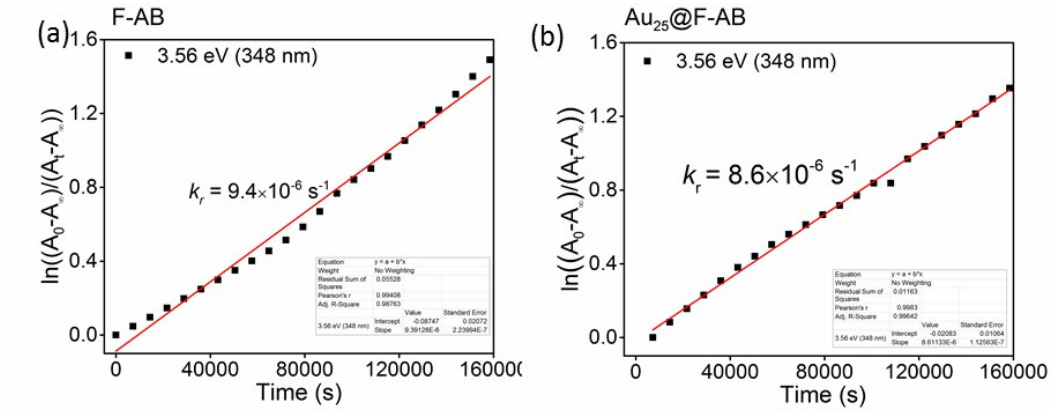

Figure S3. First-order kinetics of thermal *cis-to-trans* isomerizations of (a) F-AB and (b) Au_{25}@F-AB in dichloromethane solution at room temperature

Table S1 Activation energies (E_a), pre-exponential factor (A), and first-order kinetic rate constant (k_r) for *cis-to-trans* thermal isomerizations of different azobenzene (AB) derivatives

AB-derivatives	E_a (kJ/mol)	A (s^{-1})	K_r (s^{-1})	Isomerization time ratio
Free AB@gas	66.9			
Free AB-$CONH_2$@solution[a]	90.0 [a]	1.56×10^{10} [a]	2.1×10^{-6} [a]	
Free F-AB@solution	90.0 [a]	5.61×10^{10}	9.4×10^{-6}	1.0
Au_{25}@F-AB@solution	90.0 [a]	5.14×10^{10}	8.6×10^{-6}	1.1

[a] Data taken from Ref: S. Samai, D. J. Bradley, T. L. Y. Choi, Y. Yan and D. S. Ginger, *J. Phys. Chem. C*, 2017, **121**, 6997-7004.

3. The potential energy curve of biphenyl torsion angle in R-AB

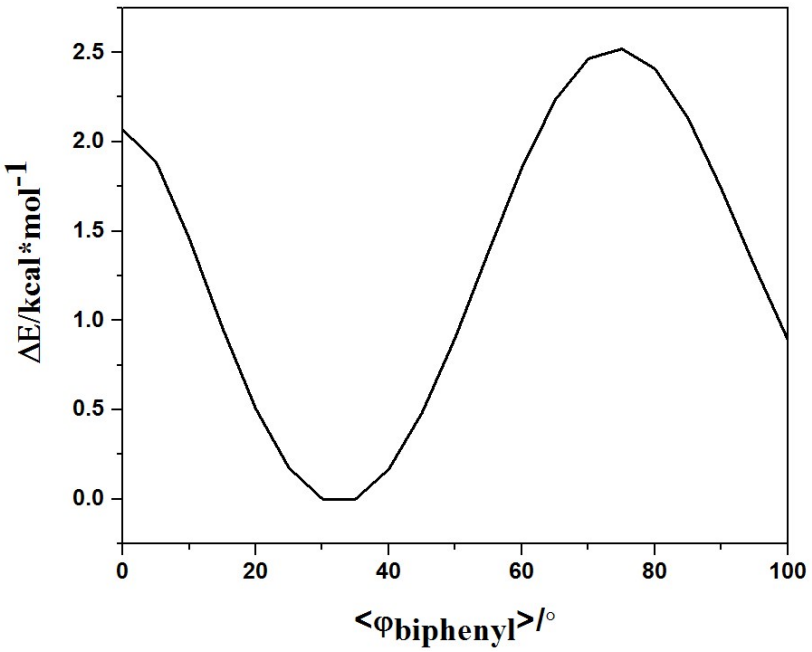

Figure S4. The potential energy curve of biphenyl torsion angle in R-AB

4. Time evolution of Au_{center}-C_{top} distance along MD trajectory of single Au@AB system

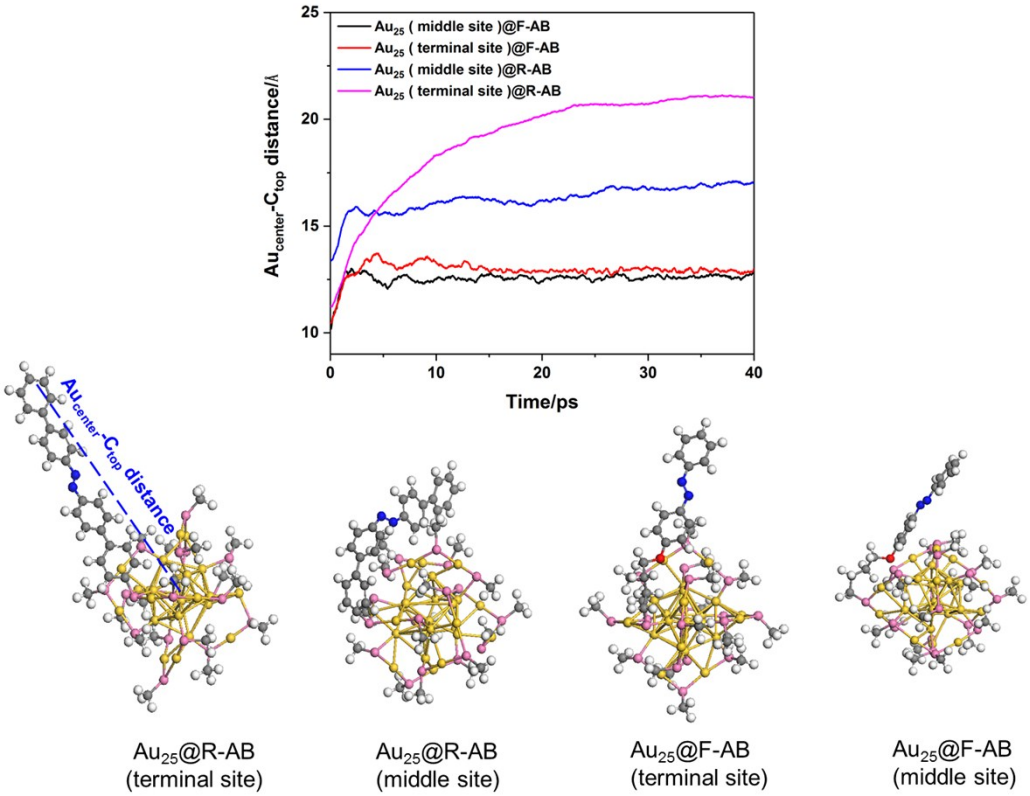

Figure S5. Time evolution of Au_{center}-C_{top} distance along MD trajectory of single Au@AB system.

5. The standard deviation of C-N=N-C dihedral of diverse Au@ AB SAMs systems

$$\text{the standard deviation} = \sqrt{\frac{1}{N}\sum_{i=1}^{N}\left(\varphi_i - \langle\varphi\rangle\right)^2}$$

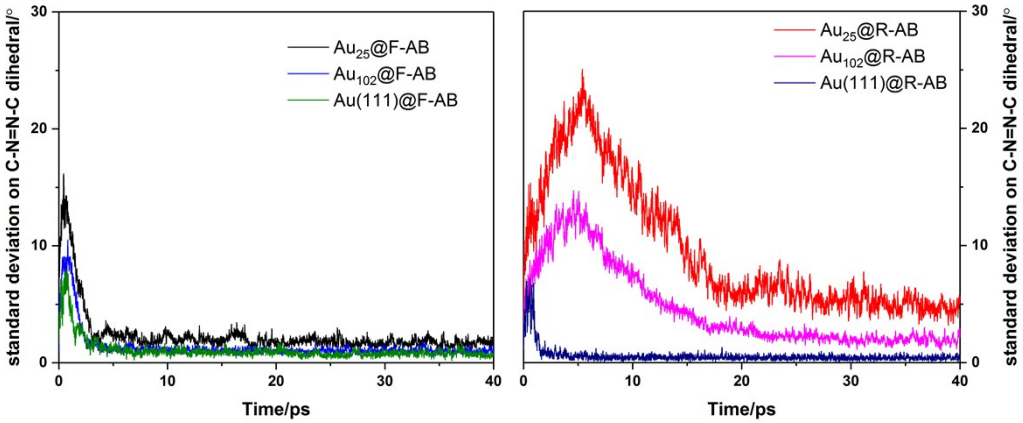

Figure S6. The standard deviation of C-N=N-C dihedral of diverse Au@ AB SAMs systems

6. The time evolution of order parameter during the switching process of six Au@AB monolayers

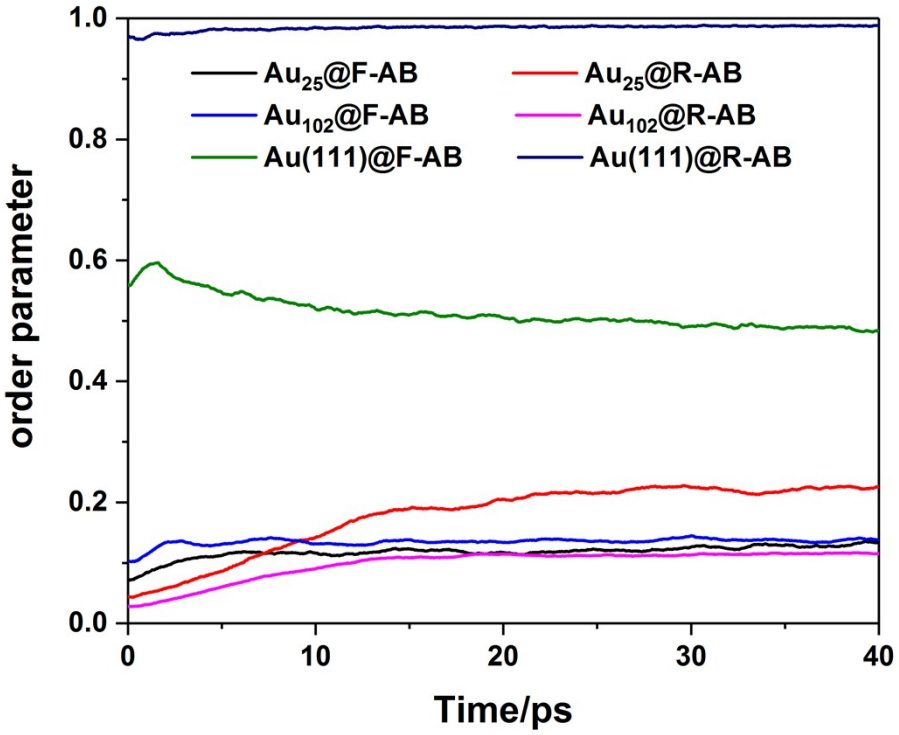

Figure S7. The trajectory of order parameter during the switching process of six azobenzene self-assembly monolayer on Au substrate

7. The trajectory of the average C-N=N-C torsion angle of single R-AB within NAMD and

CHARMM36.

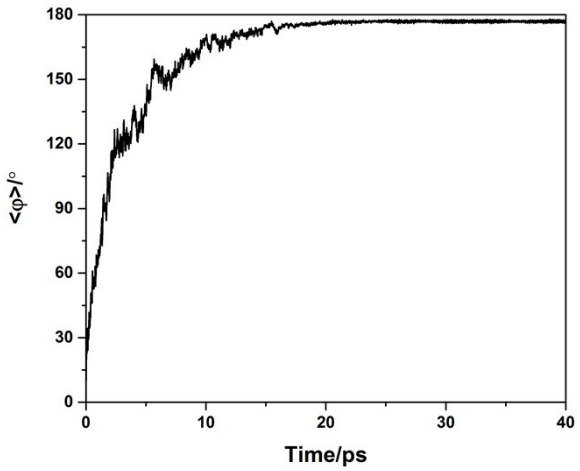

Figure S8. The trajectory of the average C-N=N-C torsion angle of single R-AB within NAMD and CHARMM36.

8. The trajectory of the average C-N=N-C torsion angle of single R-AB under potential energy

based switching functions

A different switch model, quoted from the reference 31 and based on the energy difference between S_1 and S_0, is also implemented in nonadiabatic simulation of azobenzene. The transition probability is defined as

$$P = \kappa e^{\chi\left(E_{S_1} - E_{S_0}\right)} + P_{ini}$$

Table S2. The quantum yields for different variable sets of energy-based switching function

	K	χ	P_{ini}	Quantum yield
Set1	3.0	-0.2	0	0.20
Set2	3.0	-0.1	0	0.36
Set3	1.3	-0.1	0.2	0.74
Set4	1.3	-0.1	0.1	0.60

Four different variable sets are explored. Set1 and Set2 are the same as the ones in reference 31, whilst the Set3 and Set4 are newly defined. Fifty independent simulations are performed for each set. The average C-N=N-C dihedral trajectories are shown as Figure S9, in which the quick back-and-forth switches are found. It should be mentioned that the results obtained from the potential energy based switching functions are highly sensitive to the variables. With the increase of *K*, χ, and P_{ini}, the quantum yields become higher and the final *trans* conformation is more planar.

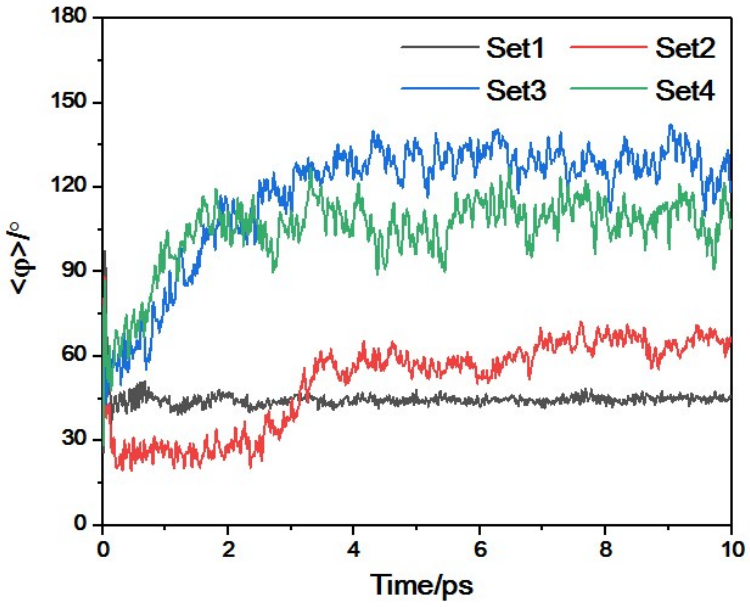

Figure S9. The trajectory of the average C-N=N-C torsion angle of single R-AB under potential energy based switching functions with different variable sets.